Complementary Capillary System Integrated Microneedles for Autonomously Localized Therapeutics Loading

Sangwook Chu, *Member, IEEE*, Nikhil Uplekar, Sanwei Liu, and Reza Ghodssi, *Fellow, IEEE*

***Abstract*— This work presents novel solid microneedles (MNs) integrated with a complementary capillary system (CCS) that enables autonomous localization of therapeutic loading. The CCS-MN, realized by 3-D direct-laser-writing (DLW), displays a double-stacked cone structure with a unique top cone consisting of opposing capillary actions: 1) external/internal capillary channels for rapid wicking/loading of liquid contents, respectively, and 2) a hydrophobic doubly-reentrant structure located at the bottom circumference for autonomous liquid confinement at the MN tip. A 2 × 2 CCS-MN array achieved robust skin penetration, withstanding 90 mN force while penetrating 300 μm into porcine skin. Significantly enhanced localized liquid loading was confirmed with the integrated CCS-MN when compared to a conventional conical MN, showing a 3.3-fold increase in loaded liquid volume (10 nL vs. 3 nL) - in good agreement with the qualitative staining test on the porcine skin from the delivered dye. Combined, this work provides a unique MN design solution realized by the DLW technology that will significantly advance minimally invasive transdermal delivery platforms.**

[2020-0166]

***Index Terms*— Direct laser writing, microneedles, transdermal delivery, interfacial fluid mechanics.**

I. Introduction

THE technological innovations in both creating biocompatible and ergonomic devices and interfacing them with various tissue and cellular targets hold exciting possibilities for engineering, modulating, and ultimately enabling therapeutic benefits in a broad range of body systems (e.g. digestive, nervous, immune systems, etc.), [1]–[5]. In particular, skin, as the largest immune organ, has provided the easiest route to access or connect with the body via advanced healthcare devices, driving the recent growing interest in utilizing wearable devices for the advent of next-generation medical diagnostics and treatments [6].

In addition to the physiological information (e.g. temperature, heart rate, sweat biochemistry, etc.) available for daily health monitoring and/or diagnostics, the skin, rich in dendritic cells (DCs) and lymph, is a primary therapeutics/vaccine delivery site [7]. Microneedle arrays (MNAs) represent a distinct class of skin-targeting platforms, enabling minimally-invasive transdermal delivery of therapeutics and vaccines with strong efficacy [8], [9], particularly in administering vaccines to target different types of pathogenic viruses (e.g. influenza [10], measles [11], polio [12]).

Among the various types of MNAs [13], coated MNAs (vs. dissolvable-, hollow-, or poke-and-patch- MNAs) provide a mechanically robust versatile delivery system capable of loading a broad spectrum of materials, ranging from small molecules to proteins, DNA, viruses, and even microparticles [14]. The efficacy of the coated MNAs have been evaluated not only in transdermal delivery, but also for delivery via eye, vascular tissue, and the oral cavity [15]. While various deliverables can potentially be coated on solid MNA surfaces, coating of the potential deliverables onto MN surfaces with high uniformity and selectivity has been a challenging task, primarily owing to the 1) limited surface area for sufficient dosage, and 2) the need for both optimization in surface energy and viscosity of carrier liquids as well as the specifically designed instruments (e.g. screening masks, ink-jet printer) for controlled liquid introduction onto MNs [16].

This work leverages the state-of-the-art 3-D direct laser writing (DLW) technology to realize system-level integration of the 3-D capillary components into MNs, ultimately to enable highly efficient and self-localizing therapeutics loading. The complementary capillary system integrated microneedle (CCS-MN) design developed in this work allowed autonomous localization of liquids carrying potential deliverables with a consistent 10 nL liquid loading per CCS-MN (compared to a 3 nL loading with conventional MN design). Combined with the mechanical robustness for skin penetration, this work successfully demonstrates an innovation in the system-level design of next-generation MNs capable of achieving self-localized coating of potential therapeutic deliverables.

Manuscript received May 14, 2020; revised May 28, 2020; accepted May 29, 2020. Date of publication June 12, 2020; date of current version October 7, 2020. This work was supported in part by the Biochemistry Program of the Army Research Office under Grant W911NF-17-1-0137 and in part by the Maryland Nanocenter and its FabLab for Support in Fabrication and Imaging Processes. Subject Editor R. Sochol. *(Corresponding author: Reza Ghodssi.)*

Sangwook Chu and Sanwei Liu are with the Institute for Systems Research, University of Maryland, College Park, MD 20742 USA (e-mail: swchu@umd.edu; swliu@umd.edu).

Nikhil Uplekar is with the Department of Electrical and Computer Engineering, University of Maryland, College Park, MD 20742 USA (e-mail: nikhilu@umd.edu).

Reza Ghodssi is with the Department of Electrical and Computer Engineering, University of Maryland, College Park, MD 20742 USA, also with the Fischell Department of Bioengineering, University of Maryland, College Park, MD 20742 USA, and also with the Institute for Systems Research, University of Maryland, College Park, MD 20742 USA (e-mail: ghodssi@umd.edu).

Color versions of one or more of the figures in this article are available online at http://ieeexplore.ieee.org.

Digital Object Identifier 10.1109/JMEMS.2020.2999255

II. Materials and Methods

A. Design and Fabrication of CCS-MN

Fig. 1a shows the CCS comprising the liquid-wicking capillary channels as well as the liquid-confining doubly reentrant overhang. The internal capillary channels displaying a volume of ~30 pL/MN were incorporated to address one of the major issues associated with coated MNAs' limited surface area for providing enough dosage. The doubly reentrant structure design has been adopted for the MNs from a previous work where an extremely limited wetting property was demonstrated, relying only on curved 3-D structures [17]. The realization of the complex MN structure was enabled via DLW (Nanoscribe Photonic Professional GT), and IP-S proprietary resin was utilized for its relatively robust mechanical property (Young's modulus: 2.6 GPa [18]) among the available photocurable resins. As shown in Fig. 1b, each CCS-MN characterized in this work displays 500 μm height (considering the epidermal depths (60 – 300 μm) for transdermal deliveries [19]) with a spacing of 300 μm between the neighboring MNs in a 2 × 2 array. The small number array of the CCS-MNs utilized in this work was sufficient for demonstration of the integrated capillary system. Printing a larger array of the CCS-MN can be accomplished using DLW for the price of a longer printing duration (i.e. the DLW of the 2×2 CCS-MN array lasted ~20 mins with the Nanoscribe Professional GT).

B. CCS-MN Characterization

Porcine skin (Animal Biotech Industries, Inc) was utilized as a biological skin model for characterizing both mechanical stability and liquid content delivery. For the mechanical characterization, thawed porcine skin was cut into approximately 1 cm × 1 cm patches for testing. The force profile during the MN penetration into the skin (at a displacement rate of 0.1 mm/s for a 0.4 mm distance) was characterized using a universal testing machine (Model 5565, Instron, MA, USA) with tensile and compressive modes containing a +/−50 N load cell.

For the characterization of MN loading and delivery, a food color dye (FD&C Blue 1, McCormick) was utilized as a model deliverable to facilitate the CCS-MN evaluation. Specifically, dye solutions in two different dilutions (undiluted vs. 97.5 % dilution in 0.01 M phosphate buffer saline (PBS)) were utilized to investigate the impact of the contact angles (CA) on capillary loading. The operation of the integrated CCS, including capillary wicking and autonomous confinement of liquid wetting, was confirmed using a high speed camera (Redlake MotionPro HS-3) to capture the rapid changes in shapes of dye solution droplets upon contact with the microneedles, and the amount of the liquid loading was quantified using optical density (OD) measurement at $\lambda = 630$ nm (absorption peak wavelength of the dye), with qualitative comparisons with level of skin coloration after delivery. For the evaluation of the delivery, the MNs remained inside the skin for 5 minutes after insertion to provide enough time for the dye solution delivery into the skin tissue via diffusion. The samples for the OD experiments were prepared by direct immersion of the loaded MNs in optical cuvettes prefilled with a buffer solution (0.01 M phosphate buffer saline, pH 7.2), and the amount of the loaded liquid volume was characterized by comparing with a standardization curve custom-generated with a known dye volume.

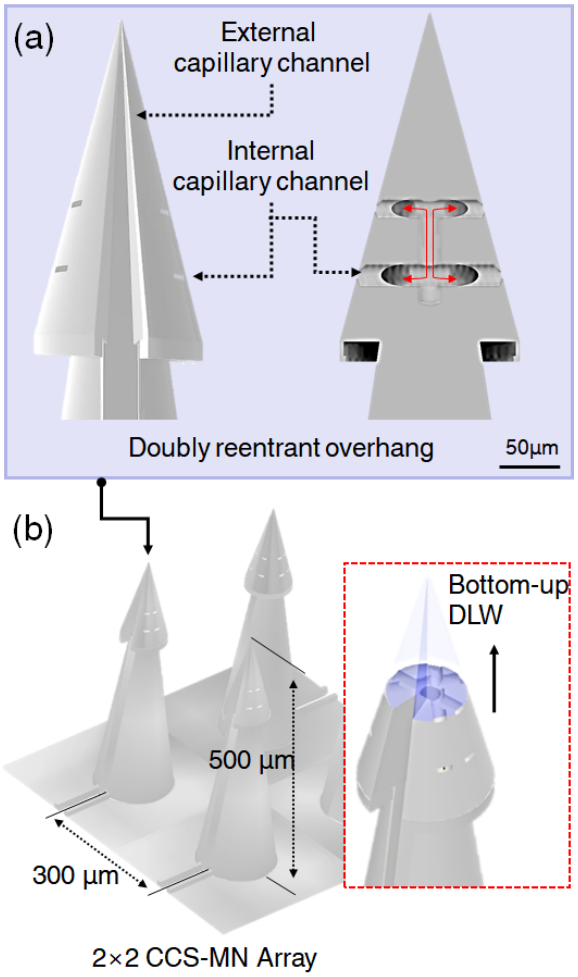

Fig. 1. Schematics of the (a) complementary capillary system (CCS) components integrated into the solid microneedle platform, and (b) the 2 × 2 CCS-MN array printed in this work via bottom-up DLW with key dimensions indicated. With the optimized printing parameters, the printing of a 2 × 2 CCS-MN array takes 20 mins.

III. Results and Discussions

A. Morphology and Robustness of 3-D Printed CCS-MNs

The SEM images shown in Fig. 2 confirm the successful 3-D construction of the double-stacked cone shaped microneedle structure. The CCS components are integrated in the top cone, which displays excellent sharpness with the MN tip measuring 1 μm in diameter. This was achieved after optimizations of the key DLW parameters including the laser power and scan speed. Both the internal and external capillary channels have been successfully formed without any noticeable structural distortion. The development step after DLW, necessary for removing excess photo-resin, was critical to completely hollow out the internal capillary channels while maintaining the good adhesion between the printed structure and substrate (glass).

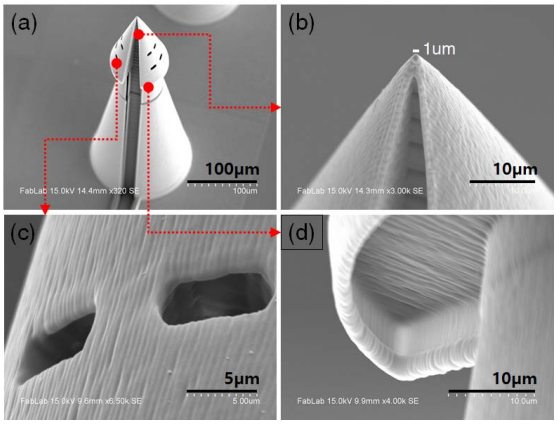

Fig. 2. SEM images of the 3-D printed CCS-MN: (a) overview of the unit CCS-MN showing the doubly-stacked cone structure with the CCS integrated at the top cone; (b) 1 μm diameter MN-tip with the external capillary channel starting at the sharp tip for rapid liquid wicking; (c) inlets to the internal capillary channels; (d) doubly-reentrant overhang at the circumference of the bottom of the top-cone, enabling self-localization of the introduced liquid.

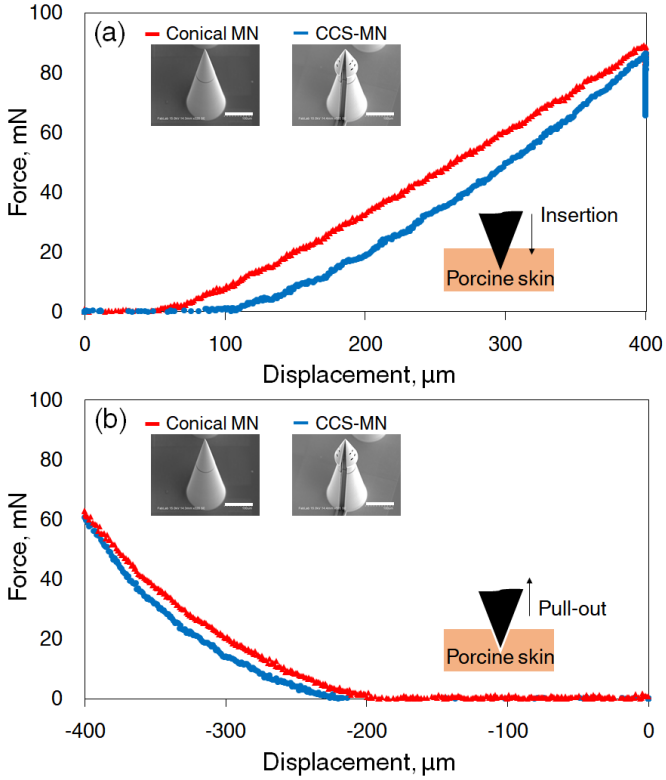

Fig. 3. Characterization of the mechanical forces experienced by the MNs (CCS-MN vs. conventional conical MN) while (a) penetrating through and (b) being removed from porcine skin. The linear characteristics observed in both measurements indicate robust penetration and easy removal of the ECCS-MN, comparable to the sharper and smoother conical MN. (Scale bars: 100 μm).

The doubly reentrant structure located at the circumference of the top cone, shown in Fig. 1d, closely resembles that of the previous reports ensuring structural hydrophobicity for autonomously confining liquid loading/coating at the top cone.

More importantly, as shown in Fig. 3, the polymeric CCS-MN showed a robust mechanical property for penetrating the porcine skin model, demonstrating robust insertion without any major disruptions/breakages as indicated by the linear change in force along the displacement, resisting up to 90 mN

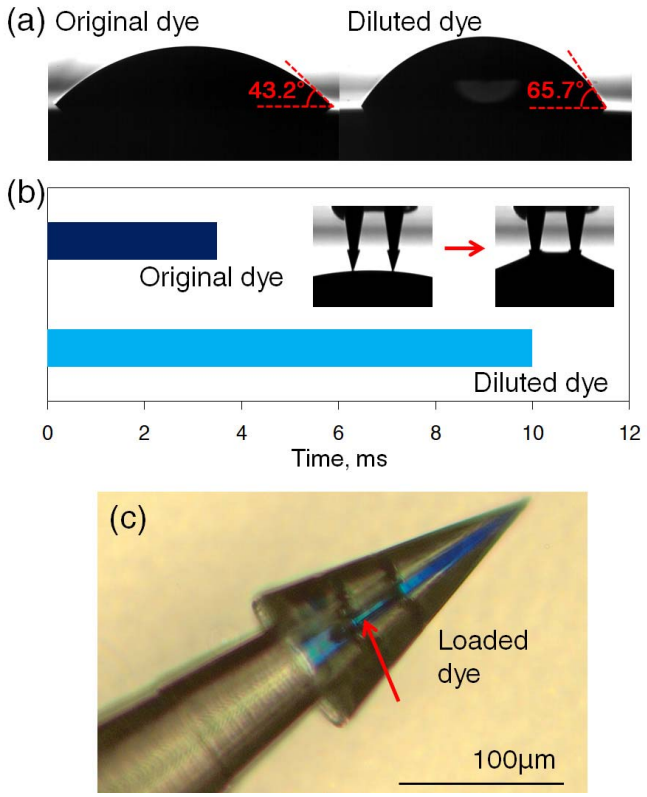

Fig. 4. Capillary loading with different dilutions of food color dye. (a) The original dye shows a relatively low surface energy CA on Au surface due to its organic compounds (e.g. propylene glycol). A 97.5 % dilution in PBS increases the CA as it becomes more aqueous. (b) The capillary loading was successful for both dilutions with the diluted dye loading at a slower rate. (c) An optical image taken after the wicking confirms the localized liquid loading at the MN-tip.

over 300 μm of penetration (effective penetration displacement). In particular, the double stacked cone structure of the CCS-MN did not induce a noticeable discrete change in insertion (Fig. 3a) or pull-out force (Fig. 3b), showing a similar change in force compared to a conventional single cone MN (Conical MN) structure. This implies a no significant tissue damage that can potentially be induced by the barb structure during the pull-out step, but this requires a further characterization using histology methods to confirm.

B. Autonomously Localized Liquid Loading

As mentioned earlier, the dye solutions in two different dilutions (original and 97.5 % dilution) were utilized in this work, each showing different surface energy as indicated by the CAs measured on Au surfaces (43.2° for original dye vs. 65.7° for diluted dye) shown in Fig. 4a. As shown in Fig. 4b, the capillary wicking event occurred more rapidly with the low surface energy liquid (i.e. the original dye containing multiple organic solvents) as compared to the diluted dye, mostly comprised of aqueous media. Specifically, the time for the respective liquid front to reach the doubly reentrant circumference of the top cone measured 3.5 ms for the original dye compared to the 10 ms for the diluted dye. Overall, it is important to emphasize that the successful wicking event with the diluted dye was confirmed, as most of the injected

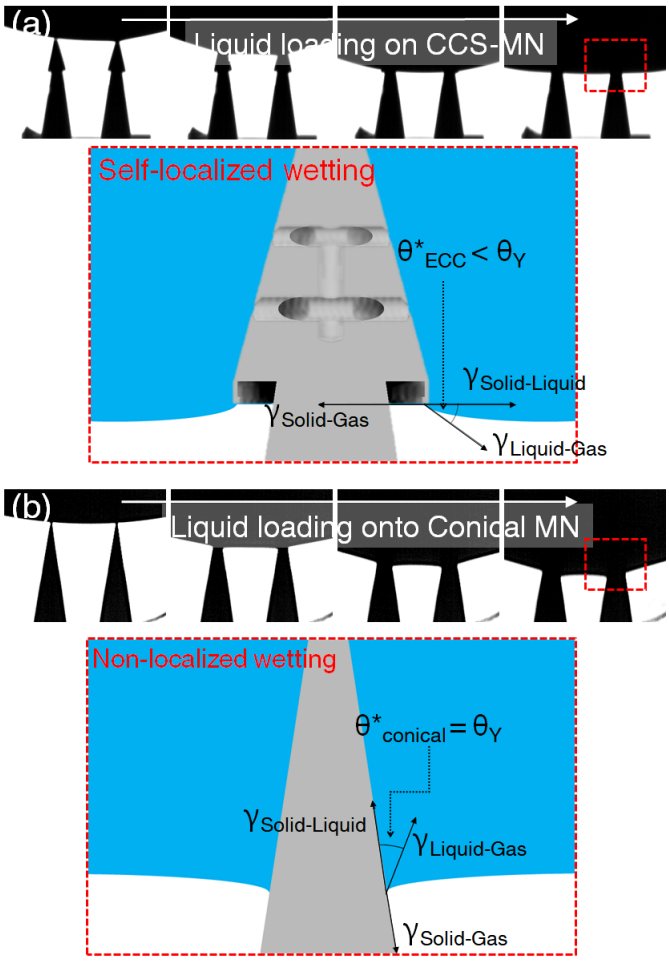

Fig. 5. (a) Liquid confinement on the CCS-MN with the doubly reentrant overhang, as opposed to the (b) continued spreading along the MN side wall on conical MN. The bottom schematics illustrate the balance between the three surface tensions at the wetting fronts and indicate that the liquid confinement at the CCS-MN can be maintained given $\theta^*_{CCS} < \theta_Y$ (Young's CA).

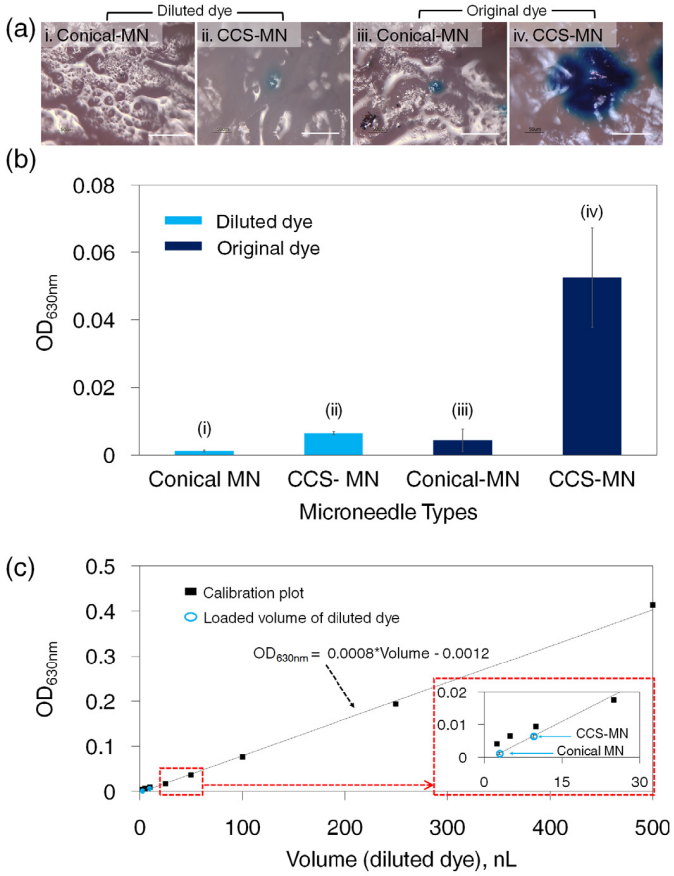

Fig. 6. Comparisons of (a) skin colorations (scale bar: 100 μm) and (b) OD_{630nm} measurements (n = 3) confirming the enhanced liquid loading/delivery with the CCS-MNs compared to conical MNs. (c) The loaded liquid volume is estimated to be 10 nL for the 2×2 CCS-MN array, compared to 3 nL for the conical MN.

therapeutics or vaccines are stored in aqueous media. The successful loading of the dye on the CCS-MN was further confirmed by a microscope image shown in Fig. 4c.

More importantly, the autonomous confinement of the liquid loading to the top cone was achieved by successful incorporation of the doubly reentrant structure. As compared in Fig. 5, the liquid-confinement observed at the doubly reentrant overhang on the CCS-MN (Fig. 5a), as opposed to the conical MN (Fig. 5b), confirms the completion of the integrated complementary system that enables autonomous localization of MN liquid loading. The enabling mechanism can be explained by the diagrams shown in red dotted boxes of Fig. 5a and 5b ($\gamma_{Solid-Liquid}$, $\gamma_{Solid-Gas}$, and $\gamma_{Liquid-Gas}$ refers to surface tensions at the respective interfaces). The continuously curved microstructures along the doubly reentrant overhang design enable apparent CA (θ^*) of the liquid meniscus at the spreading front to remain below the Young's CA (θ_Y) in ambient conditions, ultimately providing overall limited wetting characteristics. For further details behind the structural hydrophobicity please refer to [17].

C. Controlled Skin Delivery

In order to evaluate the enhanced liquid loading and delivery with the CCS-MN developed in this work, control MN samples displaying a conventional conical structure (i.e. single cone design with the absence of the top cone in CCS-MN) were utilized for comparison. Fig. 6a compares top-down optical microscope images taken from porcine skin after the delivery of the loaded dye contents using the respective MNs. The CCS-MN showed more dense skin coloration with the delivered dye contents compared to the conical MNs for both original and diluted dye cases, indicating the effective function of the embedded capillary channels for increasing the loaded liquid contents. When characterized using OD measurements for quantification of the enhancement, the difference in OD between the two different MNs was larger when loaded with the original dye compared to the diluted dye. This is most likely attributed to the lower surface energy of the original dye which drives the liquid to stay on the MN surface rather than getting pulled back upon separation of the source droplets after MN loading.

The volume of the diluted dye loaded onto CCS-MN was analyzed using a calibration plot, as shown in Fig. 6c. The results indicated that the CCS MN carried ~3.3 fold more

of the dye solution compared to the conical MN (10 nL vs. 3 nL). While this is a significant increment factor enhancing potential therapeutics/vaccine dosage range, the increment did not correspond with the designed volume of the capillary channels, which was in the pico-liter range. This implies the need of further characterization for a better understanding of the role of the internal capillary channels in enhancing the overall liquid loading volume.

IV. Conclusion

In this work, a novel complementary capillary system (CCS) integrated into a conventional solid MN design has been demonstrated, enabling autonomous localization of liquid loading/coating on MNs for the next-generation minimally-invasive therapeutic/preventive applications. This work leveraged a state-of-the-art 3-D printing technology (DLW with Nanoscribe Professional GT) for realizing complex 3-D capillary structures on MNs. With the optimized printing process parameters, the Nanoscribe printed a 2×2 array of the CCS-MN in 20 mins with excellent structural fidelity, closely replicating the 3-D computer aided designs (CAD) with 1-μm resolution. The characterization of both liquid wicking and confinement confirmed successful integration of the CCS into MNs, enabling autonomous localization of an aqueous media carrier for therapeutics/vaccines—which can potentially eliminate the need for manufacturing tools and equipment (e.g. screening masks, ink-jet printer) for achieving the same result. Combined with the robust mechanical property and the enhanced liquid loading capability of the CCS-MN, the authors believe that this work provides and enables a MN design strategy for the development of the next generation of therapeutics/vaccine delivery devices.

The authors should note that the 3-D printing technology utilized in this work is not an ideal choice for manufacturing MN arrays, as of today, due to its relatively low throughput nature compared to conventional high-throughput manufacturing methods utilized for MNs, including highly parallel microfabrication processes for micro-molding techniques. The DLW technology will need to incorporate additional laser sources or advanced optical system configurations to achieve a parallel printing process in order to compete with or lead the conventional 3-D micromanufacturing techniques. Knowing that the mechanical property of the 3-D printed resin is robust enough for skin penetration, the advanced DLW technology will provide an unprecedented route not only for incorporating enabling structures into MN arrays but also for facile integration with additional functional materials (flexible/ergonomic substrates, conductive/electrode materials), ultimately towards achieving enhanced therapeutic efficacy and disease prevention.

References

[1] J. R. Capadona, A. J. Shoffstall, and J. J. Pancrazio, "Neuron-like neural probes," *Nature Mater.*, vol. 18, no. 5, pp. 429–431, May 2019, doi: 10.1038/s41563-019-0312-9.

[2] A. J. Bandodkar and J. Wang, "Non-invasive wearable electrochemical sensors: A review," *Trends Biotechnol.*, vol. 32, no. 7, pp. 363–371, Jul. 2014, doi: 10.1016/j.tibtech.2014.04.005.

[3] K. Kalantar-Zadeh *et al.*, "A human pilot trial of ingestible electronic capsules capable of sensing different gases in the gut," *Nature Electron.*, vol. 1, no. 1, pp. 79–87, Jan. 2018, doi: 10.1038/s41928-017-0004-x.

[4] M. J. Gora *et al.*, "Tethered capsule endomicroscopy enables less invasive imaging of gastrointestinal tract microstructure," *Nature Med.*, vol. 19, no. 2, pp. 238–240, Feb. 2013, doi: 10.1038/nm.3052.

[5] S. C. P. Williams, "Under the skin of intradermal vaccines," *Proc. Nat. Acad. Sci. USA*, vol. 110, no. 25, pp. 10049–10051, Jun. 2013, doi: 10.1073/pnas.1309653110.

[6] I. C. Jeong, D. Bychkov, and P. C. Searson, "Wearable devices for precision medicine and health state monitoring," *IEEE Trans. Biomed. Eng.*, vol. 66, no. 5, pp. 1242–1258, May 2019, doi: 10.1109/TBME.2018.2871638.

[7] P. Di Meglio, G. K. Perera, and F. O. Nestle, "The multitasking organ: Recent insights into skin immune function," *Immunity*, vol. 35, no. 6, pp. 857–869, Dec. 2011, doi: 10.1016/j.immuni.2011.12.003.

[8] C. I. Shin, S. D. Jeong, N. S. Rejinold, and Y.-C. Kim, "Microneedles for vaccine delivery: Challenges and future perspectives," *Therapeutic Del.*, vol. 8, no. 6, pp. 447–460, Jun. 2017, doi: 10.4155/tde-2017-0032.

[9] K. M. Kwon *et al.*, "Microneedles: Quick and easy delivery methods of vaccines," *Clin. Experim. Vaccine Res.*, vol. 6, no. 2, p. 156, 2017, doi: 10.7774/cevr.2017.6.2.156.

[10] S. Hirobe *et al.*, "Clinical study and stability assessment of a novel transcutaneous influenza vaccination using a dissolving microneedle patch," *Biomaterials*, vol. 57, pp. 50–58, Jul. 2015, doi: 10.1016/j.biomaterials.2015.04.007.

[11] C. Edens, M. L. Collins, J. L. Goodson, P. A. Rota, and M. R. Prausnitz, "A microneedle patch containing measles vaccine is immunogenic in non-human primates," *Vaccine*, vol. 33, no. 37, pp. 4712–4718, Sep. 2015, doi: 10.1016/j.vaccine.2015.02.074.

[12] C. Edens, N. C. Dybdahl-Sissoko, W. C. Weldon, M. S. Oberste, and M. R. Prausnitz, "Inactivated polio vaccination using a microneedle patch is immunogenic in the rhesus macaque," *Vaccine*, vol. 33, no. 37, pp. 4683–4690, Sep. 2015, doi: 10.1016/j.vaccine.2015.01.089.

[13] H. L. Quinn, M.-C. Kearney, A. J. Courtenay, M. T. McCrudden, and R. F. Donnelly, "The role of microneedles for drug and vaccine delivery," *Expert Opinion Drug Del.*, vol. 11, no. 11, pp. 1769–1780, Nov. 2014, doi: 10.1517/17425247.2014.938635.

[14] H. S. Gill and M. R. Prausnitz, "Coated microneedles for transdermal delivery," *J. Controlled Release*, vol. 117, no. 2, pp. 227–237, Feb. 2007, doi: 10.1016/j.jconrel.2006.10.017.

[15] A. S. Rzhevskiy, T. R. R. Singh, R. F. Donnelly, and Y. G. Anissimov, "Microneedles as the technique of drug delivery enhancement in diverse organs and tissues," *J. Controlled Release*, vol. 270, pp. 184–202, Jan. 2018, doi: 10.1016/j.jconrel.2017.11.048.

[16] R. S. J. Ingrole and H. S. Gill, "Microneedle coating methods: A review with a perspective," *J. Pharmacol. Express Therapeutics*, vol. 370, no. 3, pp. 555–569, Sep. 2019, doi: 10.1124/jpet.119.258707.

[17] T. Liu and C.-J. Kim, "Turning a surface superrepellent even to completely wetting liquids," *Science*, vol. 346, no. 6213, pp. 1096–1100, Nov. 2014, doi: 10.1126/science.1254787.

[18] T. Frenzel, M. Kadic, and M. Wegener, "Three-dimensional mechanical metamaterials with a twist," *Science*, vol. 358, no. 6366, pp. 1072–1074, Nov. 2017, doi: 10.1126/science.aao4640.

[19] T. Waghule *et al.*, "Microneedles: A smart approach and increasing potential for transdermal drug delivery system," *Biomed. Pharmacotherapy*, vol. 109, pp. 1249–1258, Jan. 2019, doi: 10.1016/j.biopha.2018.10.078.

Sangwook Chu (Member, IEEE) received the B.S. degree in electrical and computer engineering from Hanyang University, Seoul, South Korea, in 2012, and the Ph.D. degree in electrical and computer engineering from the University of Maryland, College Park, MD, USA, in August 2018.

His Ph.D. research has focused on developing biofabrication technology using genetically-engineered Tobacco mosaic virus for developing miniature biochemical sensors and energy storage/harvesting devices that rely on electrochemical transduction. He is currently a Post-Doctoral Associate with the Institute for Systems Research, University of Maryland at College Park. He is also strongly interested in design, fabrication, and implementation of 3-D micro/nano structured materials for advancing a wide range of research areas, including energy storage/harvesting and biomedical devices.

Nikhil Uplekar was born in Boynton Beach, FL, USA, in 1997. He received the IB World School Diploma from the Atlantic Community High School, Delray Beach, FL, USA, in May 2015. He is currently pursuing the degree in computer engineering with the University of Maryland, College Park, MD, USA.

He has held internship and co-op positions with the Johns Hopkins University Applied Physics Laboratory, as well as a summer research position with the MIT Lincoln Laboratory, and a Software Engineering Internship with Amazon. He is also serving as an Undergraduate Researcher with the MEMS Sensors and Actuators Laboratory, a part of the Department of Electrical and Computer Engineering and the Institute for Systems Research. He aspires to focus his future work on the development of devices and technologies related to the medical field.

Sanwei Liu received the B.S. degree in mechanical engineering from Central South University, Changsha, China, in 2010, and the Ph.D. degree in mechanical engineering from Northeastern University, Boston, USA, in 2018, under the supervision of Prof. C. Livermore. He has been a Post-Doctoral Associate with the MEMS Sensors and Actuators Laboratory (MSAL), University of Maryland, College Park, MD, USA, since 2018. His research focuses on characterizing and engineering macroscale carbon nanotube networks using electrically induced graphitization for developing high-performance fibers with exceptional mechanical, electrical, and thermal properties. He is currently developing robust tissue anchoring structures to enable ingestible devices for long term functionalities in the gastrointestinal tract.

Reza Ghodssi (Fellow, IEEE) was the Director of the Institute for Systems Research (ISR) for eight years from 2009 to 2017. During this time, he launched a number of interdisciplinary initiatives, such as the Maryland Robotics Center (MRC) and the Brain and Behavior Initiative (BBI), aimed at enhancing the impact of ISR research efforts on society while building a more interactive faculty, staff, and student community across different disciplines in the institute. He is currently the Herbert Rabin Distinguished Chair in engineering and the Director of the MEMS Sensors and Actuators Laboratory (MSAL), Department of Electrical and Computer Engineering (ECE), the Institute for Systems Research (ISR),University of Maryland (UMD). He has more than 150 journal publications and 334 refereed conference papers, and is the co-editor of the *MEMS Materials and Processes Handbook* published in 2011. He has obtained eight U.S. patents, with another seven pending. His research interests are in the design and development of micro/nano/bio devices and systems for chemical and biological sensing, small-scale energy conversion, and harvesting with a strong emphasis toward healthcare applications.

He is also a University of Maryland Distinguished Scholar-Teacher and a Fellow of AVS and ASME. He has served as an Associate Editor for the *Journal of Microelectromechanical Systems* (JMEMS) for 11 years. He is an Associate Editor of the *Biomedical Microdevices* (BMMD).